RESEARCH ARTICLE OPEN ACCESS

Growth And Characterization Of Pure And Glycine Added Morenosite Single Crystals

J. M. Kavitha and C. K. Mahadevan
Physics Research Centre, S.T.Hindu College, Nagercoil-629 002, Tamilnadu, India

ABSTRACT
Morenosite ($NiSO_4.7H_2O$) is a hydrogen bonded crystal having a wide range of applications in various fields. In an attempt to understand the effect of glycine as an impurity on the properties of morenosite crystals, we have grown by the free evaporation method at room temperature and characterized pure and glycine added morenosite single crystals. The grown crystals were characterized structurally, mechanically, optically and electrically. The densities observed indicate that the impurity molecules have entered into the crystal matrix. The grown crystals exhibit good optical transparency in the wavelength range 210-1100 nm. The second harmonic generation measurements indicate that they are nonlinear optically active. Results of microhardness measurements follow the normal indentation size effect. Electrical (AC and DC) measurements indicate that the grown crystals exhibit a normal dielectric behaviour and the electrical conduction is understood to be due to the protonic movement. The present study indicates that glycine addition plays an important role in reducing the dielectric constant ε_r value significantly to make morenosite crystals low-ε_r value dielectric materials, expected to be useful in the microelectronics industry.
Keywords **-** Crystal growth, Electrical properties, Mechanical properties, Morenosite crystals, Optical properties, Single crystals, X-ray diffraction

I. Introduction

The mineral morenosite (nickel sulphate heptahydrate, $NiSO_4.7H_2O$) is a hydrogen bonded single crystal and is isomorphous with goslarite (zinc sulphate heptahydrate, $ZnSO_4.7H_2O$) and epsomite (magnesium sulphate heptahydrate, $MgSO_4.7H_2O$). These three minerals crystallize in the orthorhombic crystal system with tetramolecular unit cells having the space group $P2_12_12_1$. The structure consists of an octahedron formed by Ni^{2+}/ Zn^{2+}/ Mg^{2+} bonded to six water (H_2O) molecules and a tetrahedron formed by S^{6+} ion bonded to four O^{2-} ions. One additional water molecule participates in linking these structural elements with a network of weak hydrogen bonds. This interstitial seventh water molecule is easily lost at near ambient temperature to leave the material hexahydrated.

Morenosite is a chemical agent and is used for manufacturing of batteries, in fungicide mixtures, for production of catalysts, in food and oil industry, and in perfumery industry. Morenosite crystal is of emerald-green colour. The unit cell parameters [1] are : a=11.86, b=12.08 and c=6.81Å. It is soluble in water and the solubility at room temperature (at 30°C) is 77.5g/100 ml of water. The molecular weight, mean refractive index and density are 280.88, 1.483 and 1.948 g/cc respectively [2]. Pure and doped morenosite single crystals have been grown at low temperatures from aqueous solutions [3-5]. Ptasiewiez-Bak et al. [6] have determined the charge density distribution in $NiSO_4.7H_2O$ single crystals.

The SO_4 group in $NiSO_4.7H_2O$ may be considered similar to the PO_4 group (having tetrahedral geometry) in $NH_4H_2PO_4$ (ADP) and KH_2PO_4 (KDP). Mahadevan and his co-workers [7,8] have reported the possibility of reducing the dielectric constant value by adding simple organic molecules like urea and L-arginine to KDP. The electrical properties of tris(thiourea)zinc(II) sulphate (ZTS) have some similarities to those of KDP[9]. Considerable interest has been shown by several investigators in studying the effect of impurities (both inorganic and organic) on the nucleation, growth and physical properties of some hydrogen-bonded crystals like KDP and ADP and obtained several useful results. But, only limited studies have been done on morenosite crystals.

Aiming at discovering new useful materials, in the present study, we have grown morenosite single crystals by the free evaporation method and investigated the effect of glycine (a simple and interesting amino acid) as an impurity (added in the morenosite solution used for the growth of crystals) with impurity concentration ranging from 2000-10000 ppm (i.e. 0.2 - 1.0 mole%) on the properties of morenosite. A total of six crystals were grown and characterized. The results obtained are reported herein and discussed.

II. Experimental Details

2.1 Growth of single crystals

Analytical reagent (AR) grade samples of $NiSO_4.7H_2O$ and glycine along with double distilled water were used in the present study. Aqueous

solution of the required salt (pure or glycine doped) was prepared at a supersaturated concentration and taken in the nucleation cell (corning glass vessel) and allowed to equilibrate at the desired temperature. The crystals were grown in the unstirred condition. Small crystals appeared in the beginning due to slow evaporation and grew larger in considerable finite time. Best crystals were selected from this and used for the characterization measurements. The temperature and volume were kept constant respectively at 30°C and 25ml for all the crystal growth experiments. Crystals were grown from pure ($NiSO_4.7H_2O$) and five impurity (glycine) added (with impurity concentrations, viz. 0.2, 0.4, 0.6, 0.8 and 1.0 mole%) solutions. Concentration programming was done to get good morenosite crystals by using various supersaturated concentrations between 1.8 and 2.5M. 2.2 M solution gave good morenosite single crystals. This concentration was considered for growing the glycine added morenosite single crystals.

2.2. Characterization

Densities of the grown crystals were determined by using the floatation method [10,11] within an accuracy of ± 0.008 g/cm^3. Carbon tetrachloride of density 1.594 g/cm^3 and bromoform of density 2.890 g/cm^3 are respectively the rarer and denser liquids used. Fourier transform infrared (FTIR) spectra were recorded by the KBr pellet method for all the six grown crystals in the wave number range 400-4000 cm^{-1} by employing a SHIMADZU spectrometer. X-ray powder diffraction (PXRD) data were collected using an automated X-ray powder diffractometer (PANalytical) with monochromated Cu Kα radiation (λ = 1.54056 Å) in the 2θ range 10-70 °. The reflections were indexed following the procedures of Lipson and Steeple [12]. Lattice parameters were also determined from the indexed data.

The UV-Vis-NIR transmittance spectra were recorded for all the six grown crystals (dissolved in water) in the wavelength range 190-1100 nm by using a Lambda-35 spectrophotometer. The second harmonic generation (SHG) property was tested for all the six grown crystals by passing the output of Nd-YAG Quanta ray laser (with fundamental radiation of wavelength 1064 nm) through the crystalline powder sample (Kurtz and Perry method [13]). Vicker's hardness measurements were carried out on all the six grown crystals using a SHIMADZU HMV2 microhardness tester.

The DC electrical conductivity measurements were carried out to an accuracy of ±2.5% for all the six grown crystals in the present study along the c-direction (major growth direction) at various temperatures ranging from 35-80 °C by the conventional two-probe method using a million megohm meter in a way similar to that followed by Mahadevan and his co-workers [14-16]. The above temperature range was considered due to the thermal instability of these crystals beyond about 85 °C. Temperature was controlled to an accuracy of ±1 °C and the observations were made while cooling the sample crystal. Crystals with large surface defect-free (i.e. without any pit or crack or scratch on the surface, tested with a travelling microscope) size (> 3 mm) were selected and used. The extended portions of the crystals were removed completely and the opposite faces were polished and coated with good quality graphite to obtain a good conductive surface layer. The dimensions of the crystal were measured using a travelling microscope (Least count=0.001 cm). The DC conductivity (σ_{dc}) of the crystal was calculated using the relation:

$$\sigma_{dc} = d_{crys} / (R\, A_{crys}) \quad (1)$$

where R is the measured resistance, d_{crys} is the thickness of the sample crystal and A_{crys} is the area of the face of the crystal in contact with the electrode.

The capacitance (C_{crys}) and dielectric loss factor (tanδ) measurements were carried out to an accuracy of ±2% by the parallel plate capacitor method using an LCR meter (Systronics make) with a frequency of 1kHz at various temperatures ranging from 35-80 °C along the c-direction in a way similar to that followed by Mahadevan and his co-workers [20-22]. The required sample crystals were prepared as in the case of DC conductivity measurements. Here also, the observations were made while cooling the sample crystal and the temperature was controlled to an accuracy of ±1°C. The air capacitance (C_{air}) was measured only at the lower temperature considered as the temperature variation of air capacitance was found to be negligible. As the sample crystal area was smaller than the plate area of the cell, the dielectric constant of the crystal (ε_r) was calculated using Mahadevan's formula [17,18]:

$$\varepsilon_r = [A_{air}/A_{crys}][[C_{crys}-C_{air}[1-A_{crys}/A_{air}]]/C_{air}] \quad (2)$$

where C_{crys} is the capacitance with crystal (including air), C_{air} is the capacitance of air and A_{air} is the area of the electrode. The AC electrical conductivity (σ_{ac}) was calculated using the relation:

$$\sigma_{ac} = \varepsilon_0\, \varepsilon_r\, \omega \tan \delta \quad (3)$$

where ε_0 is the permittivity of free space and ω is the angular frequency of the applied field.

III. Results and Discussion

3.1. Colour, densities and lattice parameters

All the six crystals grown are found to be stable, greenish in colour and shining. Crystals upto a maximum of 2 cm length were obtained. A rough thermal test carried out on all the six grown crystals indicates that at about 85 °C, the crystals loose slowly the shining green colour and release the water of hydration with increasing temperature. Figure 1 shows a photograph of the sample crystals grown in the present study.

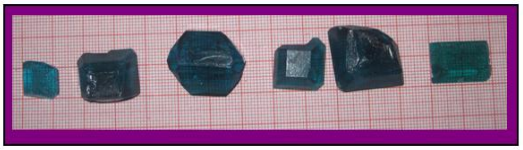

Fig.1 : Photograph of the sample crystals (From left- Pure morenosite, glycine added morenosite in the mole% 0.2, 0.4, 0.6, 0.8 and 1.0)

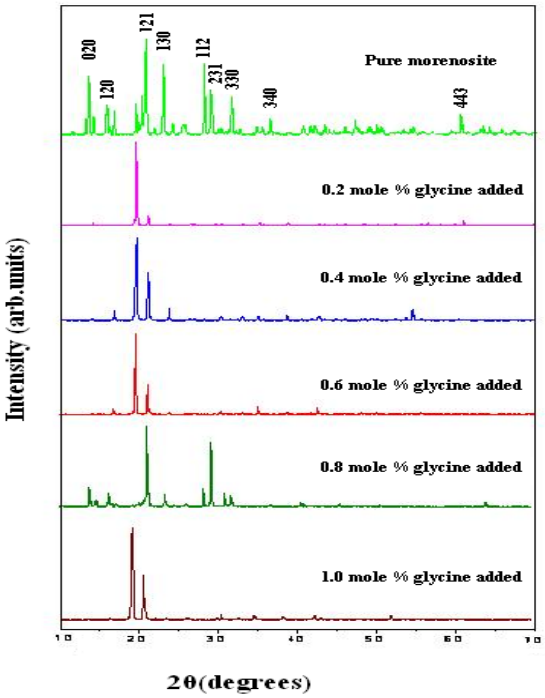

Fig.2 : The PXRD patterns observed.

The indexed PXRD patterns recorded are shown in Figure 2. Appearance of strong and sharp peaks confirms the crystalline nature of the sample crystals grown. The average densities and lattice parameters obtained are provided in Table 1.

Table 1: Densities and lattice parameters

System (with impurity concentration in the solution, mole%)	Density (g/cc)	Lattice parameters			
		a(Å)	b(Å)	c(Å)	Volume (Å^3)
Pure morenosite	1.956	11.350	12.196	6.712	929.1
Glycine added morenosite					
0.2	1.954	11.804	12.389	6.527	954.5
0.4	1.951	11.450	12.321	6.818	961.9
0.6	1.949	12.001	12.187	6.654	973.2
0.8	1.948	11.839	12.379	6.792	995.4
1.0	1.946	11.863	12.146	7.407	1067.

The average density value and lattice parameters observed in the present study for the pure morenosite crystal agree well with the literature values, confirming the identity of the substance. The observed decrease of density and increase of lattice volume caused by the impurity addition indicates that the impurity molecules have entered into the morenosite crystal matrix. Moreover, it can be seen that the density and lattice volume vary further with the increase in impurity concentration.

3.2. FTIR spectra

The FTIR spectra recorded for the grown crystals are shown in Figure 3. Significant difference could not be observed for the doped crystals as the impurity concentrations considered are small.

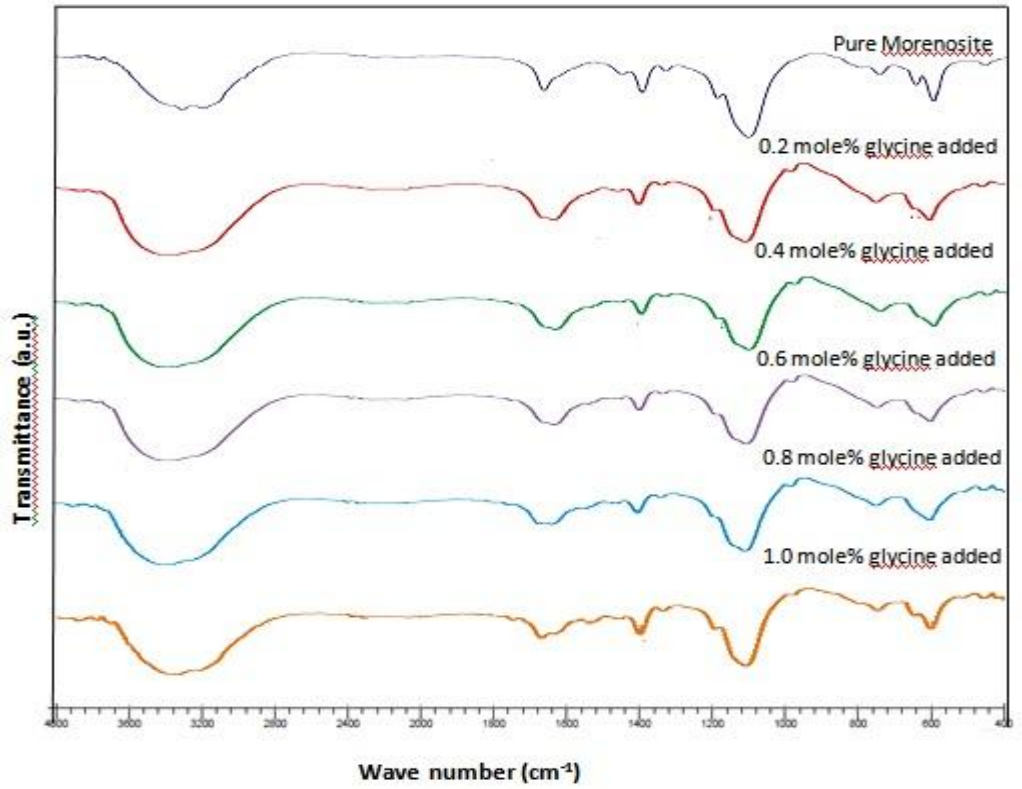

Fig.3 : The FTIR spectra observed

Four normal modes are present in the infrared region for the sulphate anion (SO_4^{2-}): a non-degenerate symmetric bending ν_1, a doubly degenerate symmetric bending ν_2, and two triply degenerate symmetric stretching and bending ν_3 and ν_4 respectively [19]. Changes in protonation, metal complexation and solvation of SO_4^{2-} can modify S-O bond length and, as a result, may change the symmetry of the anion. This leads to a shift in the vibrational bands to different wave numbers and causes the degenerate vibrations to become non-degenerate.

The broad envelope around 3379-3198 cm^{-1} indicates the presence of water and it belongs to free water symmetry stretch. The asymmetric stretch of water has been observed at 1670-1634 cm^{-1}. The bending mode of water has been observed at around 463-445 cm^{-1}. The asymmetric stretch of sulphate (ν_3) appears at 1194-1105 cm^{-1}. The bending modes of sulphate (ν_4) are positioned at around 752-730 and 654-595 cm^{-1}. The spectra observed for all the six grown crystals are similar to that reported in the literature for $MgSO_4.7H_2O$ [19-21] and $ZnSO_4.7H_2O$ [22].

3.3. Optical and mechanical properties

The UV-Vis-NIR transmittance spectra observed for the grown crystals are shown in Figure 4. All the spectra are found to be similar and they show wide transmission window with a small dip at around 390 nm in the UV-Vis-NIR region (from 210-1100 nm). This enables these crystals to be potential candidates for opto-electronic applications. Efficient nonlinear optical (NLO) crystals are expected to have optical transparency lower cut-off wavelengths between 200 and 400 nm [23]. From this it can be understood that the crystals grown in the present study can be considered as promising NLO crystals.

The second harmonic generation (SHG) efficiencies (compared to that of KDP) observed are provided in Table 2. Results obtained indicate that the crystals grown in the present study are NLO active.

The hardness behaviour is shown in Figure 5. P is the load applied and d is the diagonal length of the indentation made on the crystal surface.

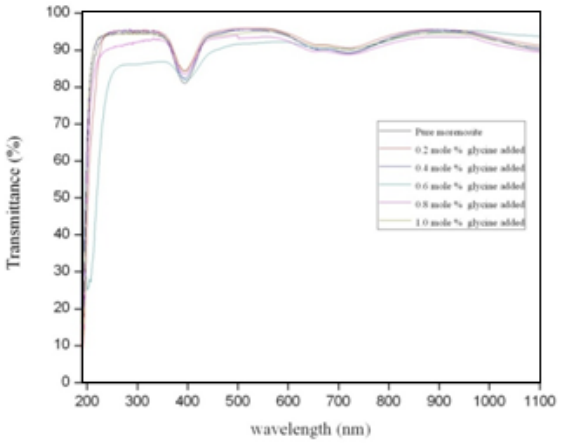

Fig.4 : The UV-Vis-NIR spectra observed

Table 2: SHG efficiencies, work hardening co-efficients (n) and DC activation energies (E_{dc})

System (with impurity concentration in the solution, mole%)	SHG efficiency (in KDP unit)	n	E_{dc} (eV)
Pure morenosite	0.93	3.17	0.572
Glycine added morenosite			
0.2	0.95	2.59	0.602
0.4	1.03	4.03	0.615
0.6	1.23	5.02	0.710
0.8	1.29	4.20	0.674
1.0	1.35	4.10	0.677

The Vicker's hardness number (H_v) is defined as

$$H_v = 1.8544\ P/d^2\ kg/mm^2 \quad (4)$$

Results obtained indicate that the H_v value increases with increasing load for all the six crystals grown in the present study. The value increases up to a load of 100 g, above which cracks start developing which may be due to the release of internal stress generation with indentation. Table 2 contains the work hardening coefficients (n) estimated from the slopes of the best-fitted straight lines of log P versus log d curves (not shown here).

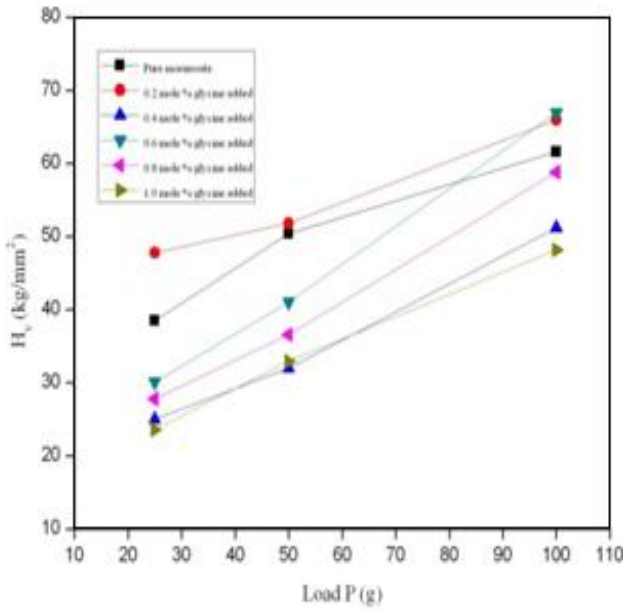

Fig.5 : The hardness behavior

Indentation size effect is the phenomenon of a solid's dependence of microhardness on the applied load at low level of testing load [24]. The Meyer's law [24] is expressed as

$$P=k_1 d^n \quad (5)$$

where k_1 is the material constant. Combining equations (4) and (5), we have

$$H_v = 1.8544 k_1 d^{n-2}$$

$$\text{Or} \quad H_v = 1.8544 k_1^{(1+2/n)}\ P^{(1-2/n)}$$

$$\text{Or} \quad H_v = b\ P^{(n-2)/n} \quad (6)$$

where $b = 1.8544 k_1^{(1+2/n)}$, a new constant. The expression shown above indicates that H_v should increase with the load if n>2. The experimental data observed in the present study agree well with this confirming the normal indentation size effect (ISE).

According to Onitsch and Hanneman 'n' should lie between 1.0 and 1.6 for hard materials and above 1.6 for soft ones [24]. The 'n' values observed in the present study are all more than 1.6 which indicates that all the six crystals grown belong to soft materials category. Thus, the experimental results observed in the present study follow the normal ISE trend.

3.4. Electrical properties

The σ_{dc}, ε_r, tanδ and σ_{ac} values obtained for pure and impurity added morenosite single crystals are respectively shown in Figures 6,7,8 and 9.

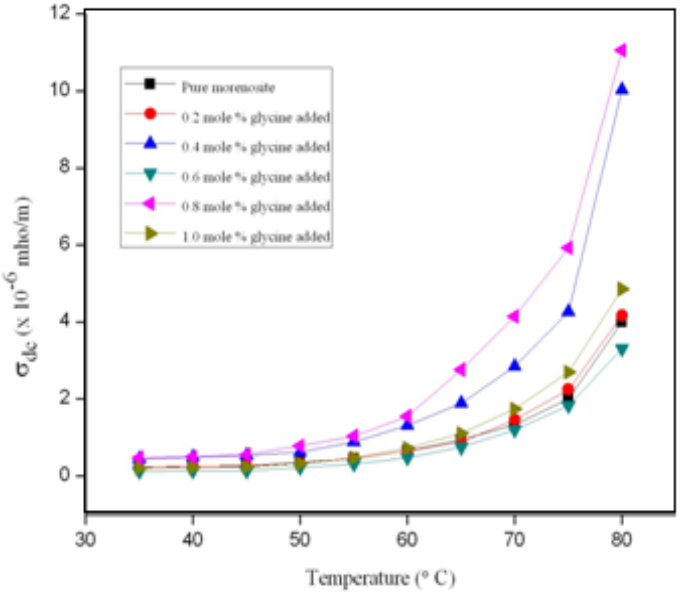

Fig.6 : DC electrical conductivities

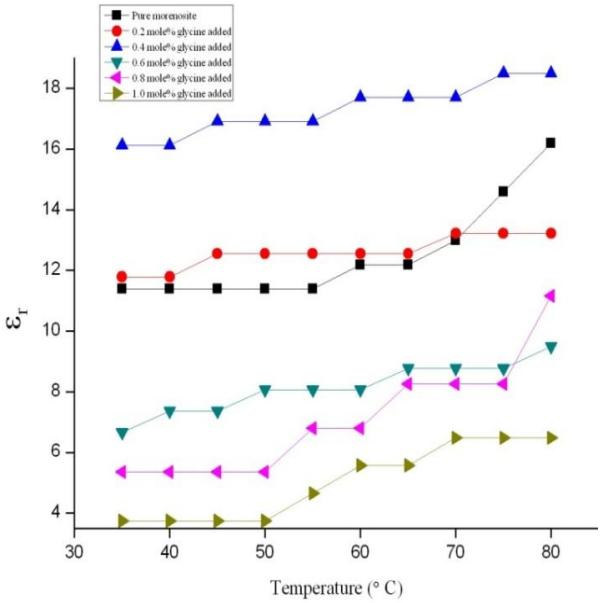

Fig.7 : Dielectric constants

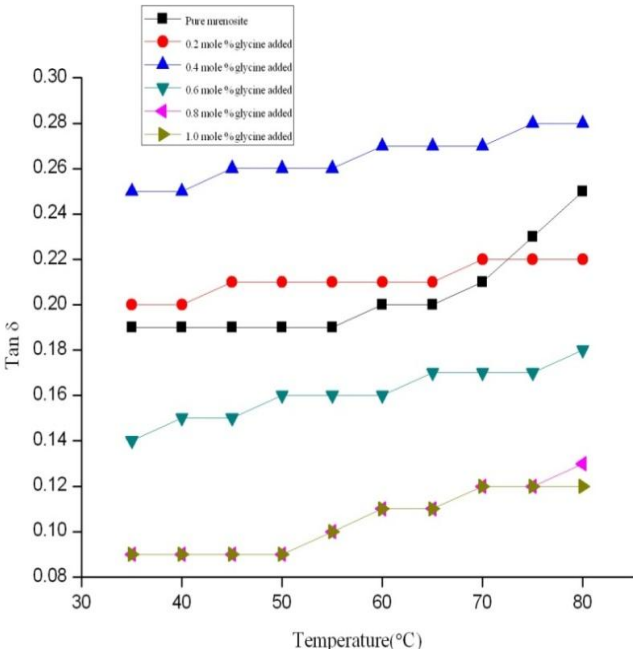

Fig.8 : Dielectric loss factors

It can be seen that σ_{dc}, ε_r, tanδ and σ_{ac} values increase with increase in temperature. However, no systematic variation is observed with the impurity concentration (taken in the solution used for the crystal growth) for all the above electrical parameters in the whole temperature range considered in the present study. 0.2 and 0.8 mole% glycine addition significantly increases the σ_{dc} values whereas 0.6 mole% significantly decreases the same. This is illustrated in Figure 10.

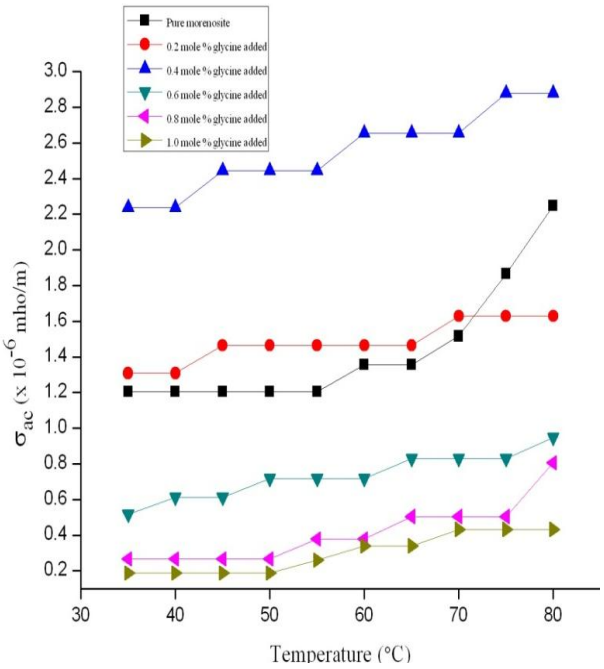

Fig.9 : AC electrical conductivities

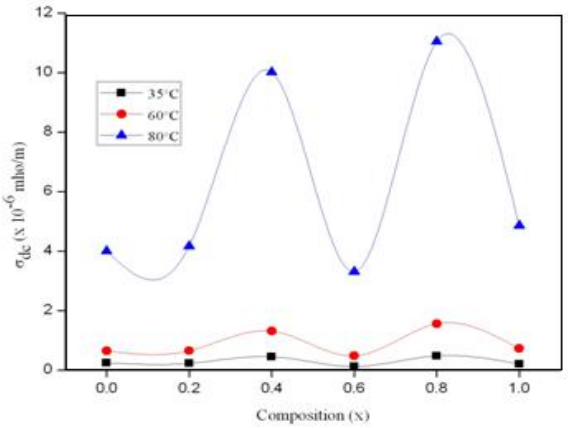

Fig.10 : Compositional dependence of σ_{dc}

Considering only the temperature range of 35-70°C, the ε_r, tanδ and σ_{ac} values increase with the increase in impurity concentration, attain the maximum for 0.4 mole % and then decrease. This is illustrated in Figure 11.

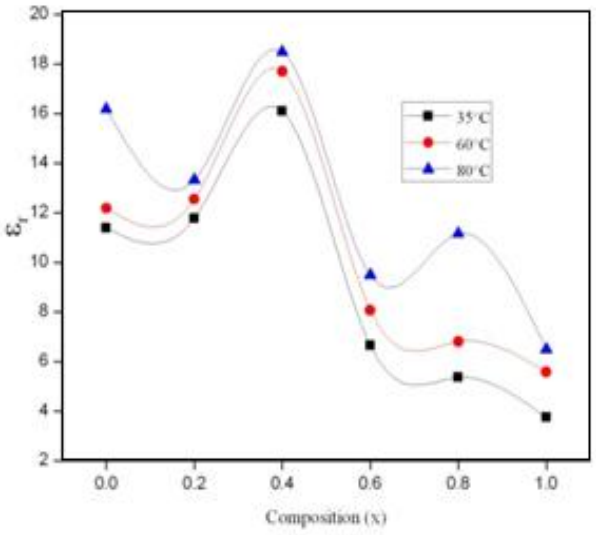

(a)

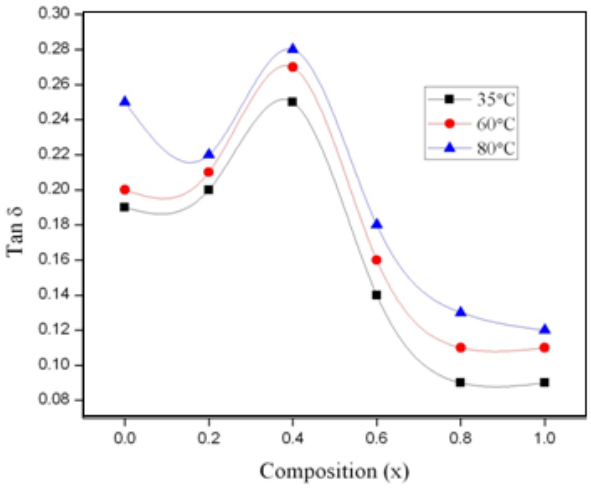

(b)

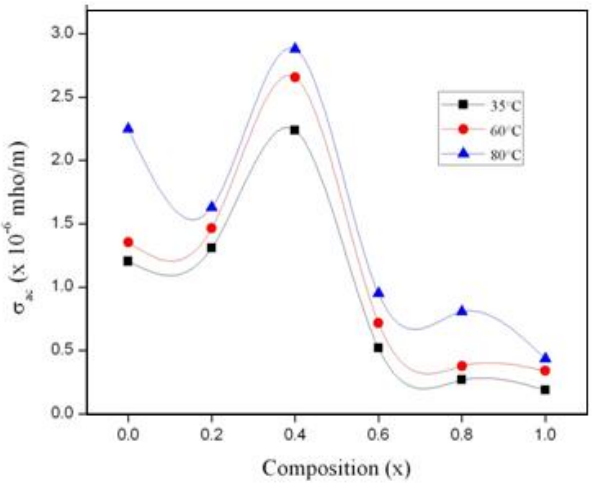

(c)

Fig.11 : Compositional dependence of: (a) ε_r, (b) tanδ and (c) σ_{ac}

The electrical conduction in dielectrics is mainly a defect controlled process in the low temperature region. The presence of impurities and vacancies mainly determine this region. The energy needed to form the defect is much larger than the energy needed for its drift. The conductivity of the crystal in the higher temperature region is determined by the intrinsic defects caused by the thermal fluctuations in the crystal [25].

The conduction region considered in the present study seems to be connected to mobility of vacancies.

If the probability of occupation of an interstice is ρ, then the probability of finding a vacant neighbour site is (1-ρ). Even for very high concentrations, of the order of 10^{20} cm^{-3}, ρ does not exceed 10^{-2} so that in real cases with concentration of interstitials of the order of 10^{15} to 10^{20} cm^{-3}, (1-ρ) ≈1 [25].

Electrical conductivity of morenosite crystals may be determined by the proton transport within the framework of hydrogen bonds. A combination of the following two mechanisms may be considered. The first mechanism is identical to the conductivity mechanism in ice also containing hydrogen bonds. According to the second mechanism, conductivity is associated with the incorporation into the crystal lattice of impurities and the formation of corresponding defects in ionic crystals. The proton conduction may be accounted for by motion of protons accompanied by a D defect (excess of positive charge). Migration of these defects may only modify electric polarization and may not change the charge at an electrode [25]. The motion of defects occurs by some kind of rotation in the bond with defects. The speed of displacement v= *va*, where *a* and *v* are the distance and frequency respectively of the jump from one bond to the other.

When the temperature of the crystal is increased there is a possibility of weakening of the hydrogen bonding system due to rotation of the hydroxyl ions in water molecules. This results in an enhanced conduction in these materials.

The mechanism of electrical conductivity in alkali and silver halide crystals is usually the motion of ions and not the motion of electrons. This has been established by comparing the transport of charge with the transport of mass as measured by the material plated out on electrodes in contact with the crystal [26].

It is assumed that the conductivity of ice is determined by the simultaneous presence of positive and negative ions and orientational defects-vacant hydrogen bonds (L-defects) and doubly occupied hydrogen bonds (D-defects). Other possible defects are vacancies and defect associates [27].

The experimental data and especially the character of the temperature dependence of conductivity allowed to understand that the conductivity of KDP crystals is determined by both thermally generated L-defects and the foreign impurities incorporated into the lattice and generating L-defects there [27]. When performing

measurements, Lokshin [28] (in the case of KDP crystals) assumed that HPO_4^{2-} ions are also responsible for the formation of vacant hydrogen bonds (L-defects). Therefore, the pH value of the initial solution, which determines its ionic composition, can be one of the most important factors that affects crystal conductivity, because the concentration of HPO_4^{2-} ions in the solution at some pH is higher by several orders of magnitude than the concentration of any other impurity [29].

From the above knowledge, it is understood that the proton transport depends on the generation of L-defects. Hence, the increase of conductivity with the increase in temperature observed for glycine added morenosite crystals in the present study can be understood as due to the temperature dependence of the proton transport. Also, the conductivity increases smoothly through the temperature range considered in the present study; there is no sharp increase that would be characteristic of a superprotonic phase transition [30].

It should be noted that the σ_{dc} values are more than the σ_{ac} values at higher temperatures as well as with higher glycine concentrations. Moreover, the increase of σ_{ac} is found to be less than that of σ_{dc} with the increase of temperature. The reason for this is not understood at present. However, it may be mentioned that when AC voltage is applied some obstruction is given by the natural and added impurities in random directions which may cause the reduction in AC conductivity at higher temperatures and with higher glycine concentrations.

Plots between ln σ_{dc} and $10^3/T$ (not shown here) are found to be nearly linear. So, the DC conductivity values were fitted to the Arrhenius relation

$$\sigma_{dc} = \sigma_{odc} \exp[-E_{dc}/(kT)] \quad (7)$$

where σ_{odc} is the proportionality constant (considered to be the characteristic constant of the material), k is the Boltzmann constant and T is the absolute temperature. The DC activation energies (E_{dc}) were estimated using the slopes of the corresponding line plots. The estimated E_{dc} values are given in Table 2. The low activation energies observed suggests that oxygen vacancies may be responsible for conduction in the temperature region considered in the present study.

The DC electrical conductivity is easily calculated [31] to be :

$$\sigma_{dc} = Ne^2a^2 / (kT\tau), \quad (8)$$

where τ is a mean jump time, perhaps different from the dipolar orientation but still given by an equation like

$$1/\tau = 1/\tau_o \exp(-E_{dc}/(kT)) \quad (9)$$

where *a* is the distance of a jump. The factor $1/\tau_o = \omega_o$ (nearly equal to $2f_D$ where f_D is the Debye frequency) is the ionic vibrational frequency around its equilibrium position and $\exp(-E_{dc}/(kT))$ is the statistical Boltzmann factor. A jump is attempted with each vibration, but only a fraction succeeds, depending on the (activation) energy E_{dc} required in order to squeeze through the barrier to neighbouring equilibrium position. N stands for the number of perfect bonds or the number of charges per unit volume. The frequency $1/\tau_o \approx 10^{13}\ s^{-1}$. Also $1/\tau \leq 10^{11}\ s^{-1}$ and $1/\tau$ will be very much smaller than this at temperatures much below the melting temperature [31].

The Debye (cutoff) frequency available in the literature [4] for the pure morenosite (determined at 25°C) is $3.247 \times 10^{12}\ s^{-1}$. The E_{dc} value obtained in the present study is 0.572 eV. The $1/\tau_o$ and $1/\tau$ values (estimated using equation (9) with the above f_D and E_{dc} values) are found to be $2.040 \times 10^{13}\ s^{-1}$ and $4.411 \times 10^3\ s^{-1}$ respectively. These values compare well with those expected by the above model. Also, the f_D value ($3.247 \times 10^{12}\ s^{-1}$ at 25°C) compares well with the frequency of the mode ($2.5 \times 10^{12}\ s^{-1}$ at 27°C) [25] assigned to oscillation modes of protons. Thus, the conduction in $NiSO_4.7H_2O$ crystals can be considered to be protonic.

It is a known fact that glycine is a simple organic substance and is expected to occupy mainly the interstitial positions. The density measurement shows a small decrease of density with the increase of impurity concentration taken in the solution used for the growth of single crystals. Moreover, the impurity concentrations considered in the present study are small. So, the glycine molecules can be assumed to replace the water molecules and ions (Ni^{2+} and SO_4^{2-}) to some extent in addition to occupying the interstitials in the morenosite crystal lattice creating a disturbance in the hydrogen bonding system. As the conduction in morenosite crystal is protonic and mainly due to the water molecules and SO_4^{2-} ions, the disturbance in the hydrogen bonding system may cause the conductivity to vary nonlinearly with the impurity concentration.

The dielectric constant of a material is generally composed of four types of contributions, viz., ionic, electronic, orientational and space charge polarizations. All these may be active at low frequencies, the nature of variations of dielectric constant with frequency and temperature indicates the type of contributions that are present in them. Variation of ε_r with temperature is generally attributed to the crystal expansion, the electronic and ionic polarizations and the presence of impurities and crystal defects. The variation at low temperature is mainly due to the expansion and electronic and ionic polarizations. The increase at higher temperatures is mainly attributed to the thermally generated charge carriers and impurity dipoles. Varotsos [32] has shown that the electronic polarizability practically remains constant in the case of ionic crystals. The increase in dielectric constant with temperature is essentially due to the temperature variation of ionic polarizability.

It should be noted that there is no significant increase of the dielectric parameters, viz., ε_r, tanδ and σ_{ac} observed with the increase of temperature at low temperatures (see Figures 7-9). However, these parameters vary significantly (although nonlinearly) with the impurity (glycine) concentration. Moreover, it is interesting to note that glycine addition (with 0.6, 0.8 and 1.0 mole% concentrations) leads to a reduction of dielectric constant significantly. The disturbance caused due to glycine addition in the hydrogen bonding system of the morenosite crystal lattice may be the reason for this.

Microelectronics industry needs replacement of dielectric materials in multilevel interconnect structures with new low-dielectric constant (ε_r) value materials, as an interlayer dielectric (ILD) which surrounds and insulates interconnect wiring. Lowering the values of the ILD decreases the RC delay, lowers power consumptions, and reduces 'cross-talk' between nearby interconnects [33].

Silica has $\varepsilon_r \approx 4.0$, in part as a result of the Si-O bonds. Several innovative developments have been made for the development of new low- ε_r materials to replace silica. Reduction in ε_r value has taken place (with non-porous and porous thin films) but with several other problems. So, there is still a need for new low-dielectric constant materials [33]. Goma et al [7] have reported reduction in ε_r value in the case of KDP added with 0.6 mole % urea. They observed at 40°C, ε_r = 2.86 along a- and 3.17 along c-directions. This illustrated that urea doping to KDP reduces the ε_r value. Moreover, material in the single crystal form would be very much interesting.

The present study indicates that glycine addition (1.0 mole %) to morenosite reduces the ε_r value from 11.391 to 3.745 in the temperature range of 35-60 °C which shows that morenosite crystal becomes interesting and useful when added with glycine. So, glycine addition leads morenosite to become a potential material useful in the microelectronics industry.

IV. Conclusions

Single crystals of morenosite added with glycine were grown by the free evaporation method and characterized structurally, optically, mechanically and electrically. Density and lattice volume variations indicate that the glycine molecules have entered into the morenosite crystal matrix. All the six grown crystals are found to be transparent in the wavelength range 210-1100nm, NLO active, mechanically soft and exhibit normal dielectric behaviour. Analysis of the DC and AC electrical conductivity data indicates that the conductivity is due to the proton transport. The present study indicates that doping morenosite with glycine leads to the discovery of promising NLO active and low-ε_r value dielectric materials.

References

[1] R.W.G.Wyckoff, *Crystal Structures (2nd edn)*, Vol.3, (Interscience, New York, 1960**)**, p.839
[2] John A. Dean (Edn), *Lange's Handbook of Chemistry (12th edn.)*, (Mc Graw Hill, New York, 1979**).**
[3] M.Theivanayagom and C.Mahadevan, *Bull.Mater.Sci.***,** *24*, 2001**,** 441.
[4] A.D.Q. Livingsta and C.Mahadevan, *Indian J.Phys.*, *76A*, 2002, 271.
[5] C.K. Mahadevan, *Physica B*, *403*, 2008, 3164.
[6] H.Ptasiewicz-Bak, I. Olovsson and G.J. McIntyre, *Acta Cryst., B53*, 1997, 325.
[7] S.Goma, C.M. Padma and C.K.Mahadevan, *Mater.Lett.*, *60*, 2006, 3701
[8] M. Meena and C. K. Mahadevan, *Cryst. Res.Technol., 43*, 2008, 166.
[9] V.N.Praveen and C.K.Mahadevan, *Indian J.Phys.*, *79*, 2005, 639.
[10] T.H.Freeda and C.Mahadevan, *Bull.Mater. Sci., 23*, 2000**,** 335.
[11] K.Jayakumari and C.K.Mahadevan, *J. Phys. Chem. Solids, 66*, 2005, 1705.
[12] H.Lipson and H.Steeple, *Interpretation of X-ray Powder Diffraction Patterns*, (Mac Millan, New York, 1970).
[13] S.K.Kurtz and T.T.Perry, *J.Appl. Phys., 39*, 1968, 3798.
[14] S.Perumal and C.K.Mahadevan, *Physica B, 367*, 2005, 172.
[15] G.Selvarajan and C.K.Mahadevan, *J. Mater.Sci.,41*, 2006, 8218.
[16] N. Manonmani, C. K. Mahadevan and V. Umayorubhagan, *Mater. Manuf. Processes, 22,* 2007, 388.
[17] M.Priya and C.K.Mahadevan, *Physica B, 403*,
[18] M.Meena, C.K.Mahadevan, *Mater.Lett., 62*, 2008, 3742.
[19] E.Ruiz-Agudo, C.V.Putnis and C. Rodriguez-Navarro, *Cryst.Growth & Des.,8*, 2008, 2665.
[20] S.Ramalingam, J.Podder and S.N.Kalkura, *J. Cryst.Growth, 247*, 2003, 523.
[21] G.Pasupathi and P.Philominathan, *Mater. Lett., 62* ,2008, 4386.
[22] J.K.Saha and J.Podder, *J. Bangladesh Acad. Sci.,35*, 2011, 203.
[23] Y.L.Fur, R.Masse, M.Z.Cherkaoui and J.F.Nicoud, *Z.Kristallogr., 210*, 1975, 856.
[24] S.Karan and S.P.Sen Gupta, *Mater.Sci. Engg., A398*, 2005, 198.
[25] J.Bunget and M.Popeseu, *Physics of Solid Dielectrics* (Elsevier, New York, 1984).
[26] C.Kittel, *Introduction to Solid State Physics (7th edn.)* (John Wiley& Sons, Singapore, 2005).

[27] L.B.Harris and G.J.Vella, *J.Chem.Phys.*, *58*, 1973, 4550.
[28] E.P.Lokshin, *Crystallogr. Rep., 41,*1996, 1070.
[29] E.P.Lokshin, *Crystallogr. Rep., 41*, 1996, 1061.
[30] D.A.Boysen, S.M.Haile, H.Liu and .A.Secco, *Chem. Mater., 16*, 2004, 693.
[31] J.R.Reitz, F.J.Milford and R.W.Christy, *Foundations of Electromagnetic Theory* (Narosa Publishing House, New Delhi, 1990).
[32] P.Varotsos, *J.Phys. Lett., 39,* 1978, L79.
[33] B.D.Hatton, K.Landskron, W.J.Hunks, M.R.Bennet, D.Shukaris, D.D.Perovic and G.A.Ozin, *Materials Today, 9(3),* 2006,22.2008, 67.